Synaptotagmin IX, a possible linker between the perinuclear endocytic recycling compartment and the microtubules

Yael Haberman[1], Elena Grimberg[1], Mitsunori Fukuda[2] and Ronit Sagi-Eisenberg[1,*]

[1]Department of Cell and Developmental Biology, Sackler School of Medicine, Tel Aviv University, Tel Aviv 69978, Israel
[2]Fukuda Initiative Research Unit, RIKEN, 2-1 Hirosawa, Wako, Saitama 351-0198, Japan
*Author for correspondence (e-mail: histol3@post.tau.ac.il)

Accepted 20 June 2003
Journal of Cell Science 116, 4307-4318 © 2003 The Company of Biologists Ltd
doi:10.1242/jcs.00719

Summary

The pericentriolar endocytic recycling compartment (ERC) is involved in receptor and lipid recycling as well as in the delivery of internalized cargo from early endosomes to the trans Golgi network (TGN). We show that synaptotagmin (Syt) IX, a member of the Syt family of proteins, localizes to the ERC and is required for export from the ERC to the cell surface. We demonstrate that rat basophilic leukemia (RBL-2H3) mast cells endogenously express Syt IX mRNA and protein. Localization studies employing fractionation on linear sucrose gradients combined with confocal microscopy by indirect immunofluorescence or stable expression of a Syt IX-green fluorescent fusion protein demonstrate that Syt IX colocalizes with internalized transferrin (Tfn) and with Rab 11 at the perinuclear ERC. Syt IX also colocalizes with tubulin at the microtubules organizing center (MTOC) and remains associated with tubulin clusters formed in taxol-treated cells. Moreover, Syt IX coimmunoprecipitates with tubulin from intact RBL cells, and chimeric fusion proteins comprising either the C2A or the C2B domain of Syt IX are able to pull down tubulin from RBL cell lysates. To study the functional role of Syt IX, we have stably transfected RBL cells with Syt IX sense or antisense cDNA and monitored the routes of Tfn internalization and recycling in cells that overexpress (RBL-Syt IX$^+$) or display substantially reduced (<90%) levels of Syt IX (RBL-Syt IX$^-$). In these cells, Tfn binding and internalization into early endosomes and the ERC are unaltered. However, recycling from the ERC to the cell surface is significantly slowed down in the RBL-Syt IX$^-$ cells. These results therefore indicate that Syt IX is involved in regulating transport from the ERC to the cell surface, and suggest that it may play a role in linking vesicles that exit the ERC with the microtubules network.

Key words: Endocytic recycling compartment, Endocytosis, Synaptotagmin, Transferrin, RBL-2H3 mast cells

Introduction

Synaptotagmins (Syts) comprise a family of structurally related proteins that are highly conserved across species from *C. elegans* and *Drosophila* to human. Synaptotagmins are present in all tissues tested so far, although they may exhibit a tissue-specific isoform distribution. Neuronal Syts have been implicated in the control of neurotransmission. Syt I and Syt II, the most abundant neuronal members, probably function as synaptic vesicle Ca^{2+} sensors (Li et al., 1995; Chapman, 2002), whereas Syt III and Syt VII, the next abundant isoforms, were suggested the role of plasma membrane Ca^{2+} sensors (Sugita et al., 2002). In a similar fashion, both Syt I and Syt IX were implicated the role of Ca^{2+} sensors in the control of dense-core vesicles exocytosis in neuroendocrine cells, such as the PC12 cells (Fukuda et al., 2002; Shin et al., 2002). Taken together, these results indicate that neuronal Syts are redundant and primarily associated with the control of Ca^{2+}-regulated exocytosis. However, the role of the non-neural members is by far less clear.

To begin exploring the role of non-neural Syt homologues, we have chosen to study the role of Syts in mast cells, specialized secretory cells that belong to the immune system. Indeed, we have previously demonstrated that rat basophilic leukemia (RBL-2H3, hereafter referred to as RBL) cells, a mucosal mast cell line, endogenously express at least three distinct Syt homologues including Syt II, Syt III and Syt V (Baram et al., 1999). Detailed analyses of Syt II and Syt III revealed that these isoforms are associated with distinct localizations and discrete functions in the RBL cells. Syt II is localized to a secretory lysosomal compartment where it functions to negatively regulate Ca^{2+}-triggered exocytosis (Baram et al., 1999) but positively regulate down-regulation of endosomal cargo, such as protein kinase Cα (Peng et al., 2002). Syt III is distributed between early endosomes and the secretory granules (SG), where it functions as a critical factor for the generation of the perinuclear endocytic recycling compartment (ERC) and the biogenesis of SG (Grimberg et al., 2003). Therefore, unlike the neural Syts, non-neural Syts are non-redundant and are functionally associated with the control of distinct steps along exo- or endocytic pathways.

Here we extend our studies and show that RBL cells endogenously express Syt IX. We show that Syt IX is localized to the perinuclear ERC, binds tubulin and is required for the export of internalized transferrin (Tfn) from the ERC to the cell

surface. We therefore propose that Syt IX may function to link exit from the recycling endosomes with the microtubules network.

Materials and Methods

Antibodies

Antibodies used included affinity purified anti-Syt IX antibodies raised in rabbits against the synthetic peptide KTPPDSSRIRQGAVC and specific for the amino terminus of Syt IX (anti-N-Syt IX) and antibodies raised in rabbits against the C2A domain of Syt IX (anti-Syt C2A-Syt IX) and purified as described previously (Fukuda et al., 2002); monoclonal antibodies against α (Sigma) or β tubulin (Santa Cruz); monoclonal antibodies directed against T7 (Novagen, Germany); monoclonal antibodies directed against Flag (Sigma); polyclonal antibodies for mannosidase II [a generous gift from Dr J. Donaldson, National Institutes of Health (NIH), MD, USA]; monoclonal anti-GFP antibodies (Roche Diagnostics); monoclonal anti-serotonin antibodies (DAKO, Denmark); polyclonal antibodies directed against $G\alpha i_2$ (AS10, a generous gift from Dr A. Spiegel, NIH); Horseradish-peroxidase (HRP)-conjugated goat anti-rabbit or anti-mouse IgG and Rhodamine or FITC-conjugated donkey anti-rabbit or anti-mouse IgG (Jackson Research Laboratories, West Grove, PA, USA).

Reagents

Fluorescein isothiocyanate (FITC)- or Texas red (TR)-conjugated human Tfn were obtained from Molecular Probes (Eugene, OR, USA). Brefeldin A, taxol, Glutathione-Sepharose, holo human Tfn and deferoxamine mesylate were from Sigma, protein A-Sepharose was from Amersham Biosciences and DEAE Dextran was from Amersham Pharmacia Biotech.

Cell culture

RBL and Cos-7 cells were maintained in adherent cultures in DMEM supplemented with 10% FCS in a humidified atmosphere of 5% CO_2 at 37°C.

Reverse transcription and PCR amplification of Syt IX cDNA

Total RNA was isolated using the TRIzol™ Reagent (Life Technologies). cDNA was synthesized for 1 hour at 42°C followed by 5 minutes at 99°C, using the Promega Reverse Transcription System kit (Promega, Madison, WI, USA). The first round of nested PCR was performed using primers A and B (A: 5′ GTACTTGGGTACCTCT-GCAG 3′; B: 5′ AGAGACTGGGAGAAAGGAGATCA 3′) and 1 μl of the reverse transcription reaction as template. For the first round of PCR, 30 cycles of 1 minute at 94°C, 1 minute at 56°C and 1 minute at 72°C were performed. One μl of the PCR product obtained and primers C and D (C: 5′ CGCGGATCCGCGATGTTCCCGGAACCC-CCGA 3′; D: 5′ GGAATCCCTCAGGGTGCAGGTATTGGC 3′) were subsequently used for a second round of PCR identical to the first, except that the annealing temperature was 55°C. The product of the second reaction was purified by agarose gel electrophoresis and ligated into BamH1/EcoR1 sites of the pcDNA3 vector (Invitrogen, San Diego, CA, USA). DH5α cells were transformed with the ligation mixture and colonies selected for sequencing.

Construction of tagged Syt IX cDNAs

Construction of T7- or Flag-Syts was performed by PCR as described previously (Fukuda and Mikoshiba, 2000). Briefly, the sequences encoding the T7 or Flag tags were inserted into the 5′-end of each Syt cDNA. To generate Flag-Syt IX-GFP the sequences encoding the Flag tag were inserted into the 5′-end of Syt IX mouse cDNA, whereas the 3′-end was ligated to the 5′-end of GFP cDNA to endcode a fusion protein. A glycine linker was inserted between Syt IX and GFP as described previously (Saegusa et al., 2002). The tagged cDNAs were subcloned into pEF-BOS or pShooter vector (Invitrogen) and verified by DNA sequencing.

Construction of GST fusion proteins

GST-Syt IX-C2A and GST-Syt IX-C2B were constructed by PCR. GST-Syt IX-C2A was constructed as described previously (Fukuda et al., 1996). GST-Syt IX-C2B was constructed using the sense primer 5′ CGCGGATCCGCGAAAGAGGAGCAGGAGAAACT 3′, the antisense primer 5′ GGAATCCCTCAGGGTGCAGGTATTGGC 3′ and RBL Syt IX cDNA as a template. The PCR product was subcloned into the BamH1/EcoR1 sites of the pGEX vector and transformed into TOP10 cells. Fusion proteins were induced by 1 mM IPTG at 30°C for 3 hours and immobilized on Glutathione-Sepharose beads.

Cell transfection

Stable transfection of RBL cells: RBL cells (8×10^6) were transfected with 20 μg of either recombinant vector (pcDNA3-Syt IX, pcDNA3-antisense-Syt IX or pShooter-Syt IX-GFP) or empty pcDNA3 vector by electroporation (0.25 V, 960 μF). Cells were immediately replated in tissue culture dishes containing growth medium (supplemented DMEM). G418 (1 mg/ml) was added 24 hours after transfection and stable transfectants selected within 14 days.

Transient transfection of RBL cells: RBL cells (6×10^7) were transfected with 40 μg of Rab 11-GFP cDNA (a generous gift from Dr M. Zerial, Max Plank Institute, Dresden, Germany) by electroporation (0.4 V, 960 μF). Cells were immediately replated in tissue culture dishes containing supplemented DMEM.

Transient transfection of Cos-7 cells: Cos-7 cells were cultured to 60% confluence and were transiently transfected using DEAE dextran/chloroquine methods with 10 μg of plasmid containing the appropriate cDNA (Aruffo and Seed, 1987).

Subcellular fractionation of RBL cells

RBL cells were serum-starved for 1 hour and incubated for 1 hour with biotin-conjugated Tfn (20 μg/ml). Cells were then fractionated as previously described (Baram et al., 1999). Briefly, RBL cells (7×10^7) were washed with PBS and suspended in homogenization buffer [0.25 M sucrose, 1 mM $MgCl_2$, 800 U/ml DNase I (Sigma-Aldrich), 10 mM Hepes, pH 7.4, 1 mM PMSF, and a cocktail of protease inhibitors (Boehringer Mannheim, Germany)]. Cells were subsequently disrupted by 3 cycles of freezing and thawing, followed by 20 passages through a 21-gauge needle and 10 passages through a 25-gauge needle. Unbroken cells and nuclei were removed by centrifugation for 10 minutes at 500 ***g*** and the supernatants subjected to sequential filtering through 5- and 2-μm filters (Poretics). The final filtrate was then loaded onto a continuous, 0.45-2.0 M sucrose gradient (10 ml), which was layered over a 0.3 ml cushion of 70% (wt/wt) sucrose and centrifuged for 18 hours at 100,000 ***g***.

Cell lysates

RBL or Cos-7 cells (1×10^7) were lysed in lysis buffer comprising 50 mM Hepes, pH 7.4, 150 mM NaCl, 10 mM EDTA, 2 mM EGTA, 1% Triton X-100, 0.1% SDS, 50 mM NaF, 10 mM NaPPi, 2 mM $NaVO_4$, 1 mM PMSF and a cocktail of protease inhibitors (Boehringer Mannheim, Germany). Following 10 minutes incubation on ice, lysates were cleared by centrifugation at 9000 ***g*** for 15 minutes at 4°C. The cleared supernatants were mixed with 5× Laemmli sample buffer, boiled for 5 minutes and subjected to SDS-PAGE and immunoblotting as described previously (Baram et al., 1999).

Immunoprecipitation

Cells were lysed in buffer A [50 mM Hepes, pH 7.4, 150 mM NaCl, 1 mM $MgCl_2$, 1% Triton X-100, 1 mM PMSF and a cocktail of protease inhibitors (Boehringer Mannheim, Germany)]. After solubilization at 4°C for 10 minutes, supernatants were cleared by centrifugation at 9000 ***g*** for 15 minutes at 4°C. Aliquots of cleared supernatants containing 500 μg protein were incubated for 18 hours at 4°C with the desired antibody. The immune complexes were captured by adding 25 μl of protein A-Sepharose (50% v/v) and incubating for 1.5 hours at 4°C. Immune complexes were washed four times with lysis buffer A, suspended in Laemmli sample buffer, boiled for 5 minutes, resolved by 10% SDS-PAGE under reducing conditions and transferred into nitrocellulose papers for Western blotting with the appropriate antibodies. Immunoblotting was performed as described previously, using the appropriate secondary antibodies. Immunoreactive bands were visualized by the enhanced chemiluminescence method according to manufacturer's instructions.

Affinity chromatography on GST fusion proteins

Cells were lysed in buffer A as described above. Aliquots of cleared supernatants containing 500 μg protein were incubated for 4 hours at 4°C with 20 μg of GST, GST-Syt IX-C2A or GST-Syt IX-C2B. At the end of the incubation period, beads were sedimented by centrifugation at 5000 ***g*** for 4 minutes at 4°C. Beads were washed 4 times with buffer A and finally suspended in 1× Laemmli sample buffer and boiled for 5 minutes and subjected to SDS-PAGE and immunoblotting.

Immunofluorescence microscopy

RBL cells (2×10^5 cells/ml) were grown on 12-mm round glass coverslips. For immunofluorescence processing cells were washed twice with PBS and fixed for 15 minutes at room temperature in 3% paraformaldehyde/PBS. Cells were subsequently washed three times with PBSCM (PBS supplemented with 1 mM $CaCl_2$ and 1 mM $MgCl_2$) and permeabilized on ice for 5 minutes with 100 μg/ml digitonin. After two washes with PBSCM, cells were permeabilized for an additional 15 minutes at room temperature with 0.1% saponin in PBSCM. Cells were subsequently incubated for 1 hour at room temperature with the primary antibodies diluted in PBSCM/5% FCS/2% BSA, washed 3 times in PBSCM/0.1% saponin and incubated for 30 minutes in the dark with the appropriate secondary antibody (Rhodamine- or FITC-conjugated donkey anti-rabbit or anti-mouse IgG, at 1/200 dilution in PBSCM/5% FCS/2% BSA). Coverslips were subsequently washed in PBSCM/0.1% saponin and mounted with Gel Mount mounting medium (Biomedica, Foster City, CA, USA). Samples were analyzed using a Zeiss laser confocal microscope (Oberkochen, Germany). The average fluorescence intensity was determined using the LSM image analysis software (Zeiss, Oberkochen, Germany).

Tfn internalization

RBL cells (mock or Syt IX sense or antisense cDNA transfected) were grown on glass coverslips, serum starved for 1 h at 37°C in DMEM supplemented with 0.2% BSA and 50 mM Hepes, pH 7.4, followed by 1 hour of incubation at 4°C with Texas Red or FITC-conjugated Tfn (50 μg/ml) to allow binding. Unbound Tfn was removed by washing with ice-cold PBS. To allow endocytosis the cells were transferred to 37°C for the desired time periods. The reaction was stopped by placing the cells on ice. Cells were subsequently processed for immunofluorescence as described above.

Tfn recycling

RBL cells (mock or Syt IX sense or antisense cDNA transfected) were grown on glass coverslips, serum starved for 1 hour in DMEM supplemented with 0.2% BSA and 50 mM Hepes, pH 7.4, followed by incubation with TR-Tfn (50 μg/ml) for 1 hour at 37°C. Cells were washed twice in PBS and unlabeled Tfn (100 μg/ml) and deferoxamine mesylate (100 μM) were added. At selected times, incubations were stopped by placing the dishes on ice and cells were processed for immunofluorescence as described above.

Data presentation

Data represent one of at least three separate experiments.

Results

Expression of Syt IX in RBL cells

An initial round of PCR with primers corresponding to positions 31 (sense) and 1510 (antisense) of Syt IX (primers A and B, under Materials and Methods) on RBL cell cDNA yielded no detectable product. However, when used as template in a second round of PCR, using primers corresponding to positions 72 and 1243 of Syt IX (primers C and D, under Materials and Methods), the nested reaction yielded a product of the predicted size of 1171 bp (Fig. 1). Sequencing of the product confirmed that RBL cells endogenously express mRNA encoding Syt IX.

To study the expression of Syt IX at the protein level we used an antibody generated against a sequence present at the amino terminal domain of Syt IX (anti-N-Syt IX) (Fukuda et al., 2002). The specificity of these antibodies was established by testing their immunoreactivity against epitope-tagged Syt isoforms that were transiently transfected into Cos-7 cells. Indeed, the anti-N-terminal antibodies decorated a 50 kDa protein that was expressed in Cos-7 cells transfected with either flag or T7-tagged-Syt IX cDNA (Fig. 2A). As expected, this 50 kDa protein could be detected on immunoblots probed with antibodies directed against the flag or T7 epitope, respectively (Fig. 2A). In contrast, the anti-N-terminal antibodies failed to exhibit any significant signal when used to probe lysates derived from mock transfected Cos-7 cells or from cells bearing other tagged Syt isoforms, including Syt I, Syt II, Syt III and Syt V (Fig. 2B).

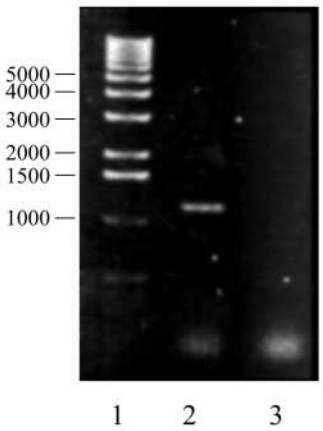

Fig. 1. PCR amplification of Syt IX cDNA. An agarose gel of the product of the second round of PCR, using for template the PCR product of RBL cell cDNA (2) or no DNA (3). The DNA size markers in bp are shown in (1).

The anti-N-Syt IX antibodies decorated three proteins of 50, 40 and 25 kDa, present in RBL cell lysates (Fig. 2C). Incubation of the antibodies with the antigenic peptide inhibited binding to all three proteins, thus indicating the specificity of binding (Fig. 2C). However, stable transfection with sense or antisense full-length Syt IX cDNAs respectively increased or decreased only the expression of the 50 and 40 kDa proteins, whereas the expression level of the 25 kDa protein remained unaltered (Fig. 2C). These results therefore confirmed that the 50 and 40 kDa immunoreactive proteins indeed corresponded to endogenously expressed Syt IX, however the 25 kDa protein is probably unrelated.

To validate further the identification of the 50/40 kDa proteins as Syt IX, RBL cells were probed with a second anti-Syt IX antibody that was raised against the C2A domain of Syt IX (anti-C2A-Syt IX) (Fukuda et al., 2002). This antibody failed to recognize any endogenous proteins (not shown), however it did bind to 50 and 40 kDa proteins present in Syt IX overexpressing cells (RBL-Syt IX$^+$), although with some preferences for the 50 kDa protein (Fig. 2D). Finally, stable transfection of the RBL cells with a GFP tagged-version of Syt IX yielded the expression of two proteins of 80 and 70 kDa which could be immunoblotted by either anti-GFP, anti-N- or anti-C2A-Syt IX antibodies (Fig. 2E). Notably, in their GFP-tagged versions, both the larger and smaller forms of Syt IX were recognized by the anti-C2A-Syt IX antibodies (Fig. 2E). We do not currently know what causes this discrepancy, however, members of the Syt family undergo post-translational modifications (e.g. palmitoylation and O-glycosylation) which may affect Syt size and immunoreactivity.

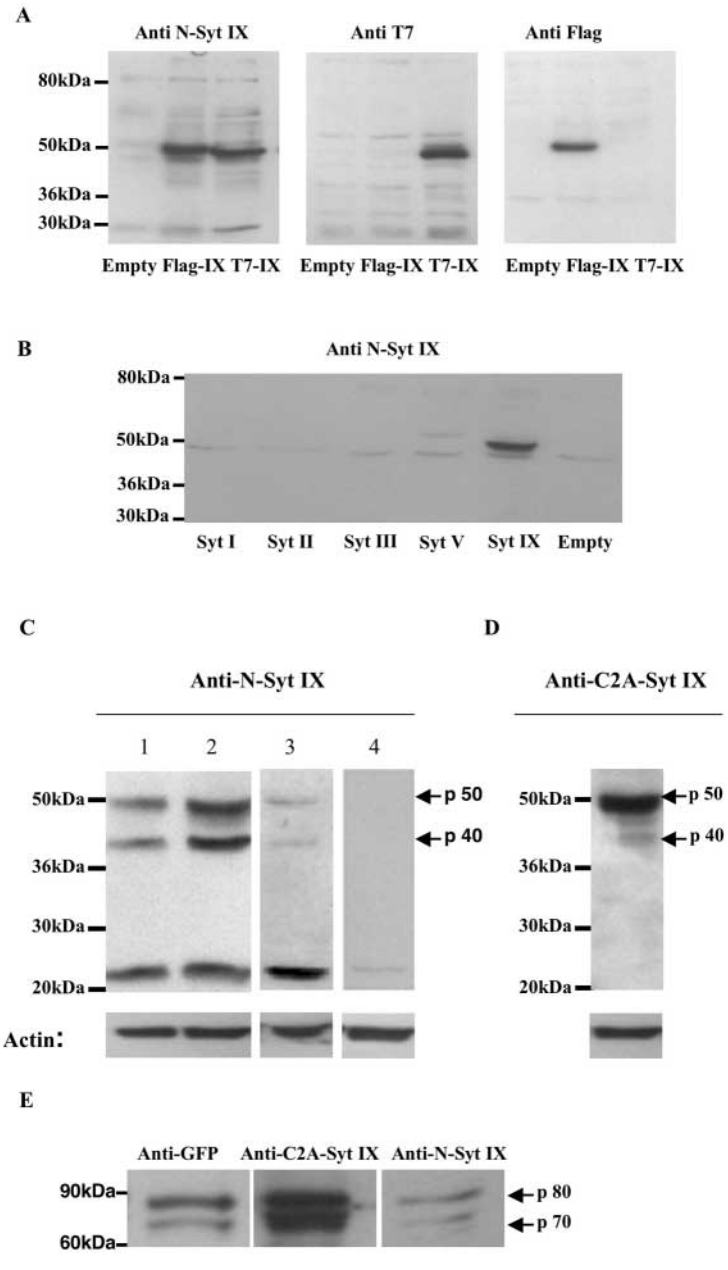

Fig. 2. Expression of Syt IX in RBL cells. (A) Cell extracts (60 μg) derived from Cos-7 cells transfected with empty vector, T7-tagged Syt IX cDNA or Flag-tagged Syt IX cDNA were resolved by SDS-PAGE and subjected to immunoblotting with anti-N-Syt IX (1 μg/ml), anti-T7 or anti-Flag antibodies. **(**B**)** Cell extracts (60 μg) derived from Cos-7 cells transfected with empty vector or with Syt I, Syt II, Syt III, Syt V and Syt IX cDNAs were resolved by SDS-PAGE and subjected to immunoblotting with anti-N-Syt IX antibodies. **(**C**)** Cell extracts (80 μg) derived from RBL cells stably transfected with either empty vector (1), or with pcDNA3-Syt IX sense cDNA, RBL-Syt IX$^+$ (2) or with pcDNA3-Syt IX antisense cDNA, RBL-Syt IX$^-$ (3) were resolved by SDS-PAGE and subjected to immunoblotting with anti-N-Syt IX antibodies in the absence (1-3) or presence (4) of the immunizing peptide (250 ng/ml). **(**D**)** Cell extracts (80 μg) derived from RBL-Syt IX$^+$ cells were resolved by SDS-PAGE and subjected to immunoblotting with anti-C2A-Syt IX antibodies (1 μg/ml). The cellular level of actin was determined to judge for equal loading. **(**E**)** Cell extracts (80 μg) derived from RBL cells stably transfected with pShooter Syt IX-GFP cDNA were resolved by SDS-PAGE and subjected to immunoblotting with anti-GFP, anti-C2A-Syt IX or anti-N-Syt IX as indicated.

Cellular distribution of Syt IX

Fractionation of RBL or RBL-Syt IX$^+$ cells on continuous sucrose gradients revealed that the endogenous 50/40 kDa proteins, detected by the anti-N-Syt IX antibodies, as well as the overexpressed 50/40 kDa proteins, detected by the anti-C2A antibodies, comigrated with fractions 19-24, at ~1.4 M sucrose (Fig. 3). These results therefore confirmed that both the endogenous and the overexpressed Syt IX protein(s) were targeted to the same cellular compartment. A small fraction of these proteins migrated at fractions 11-14 at ~1 M sucrose (Fig. 3), which contain the plasma membrane (Grimberg et al., 2003). In contrast, the 25 kDa protein that immunoreacted only with the anti-N-Syt IX antibodies comigrated with fractions 15-19 at 1.2 M sucrose (Fig. 3).

Consistent with previous results, fractions 19-24, which contain both the endogenous and the overexpressed Syt IX protein(s), also contained histamine and β-hexosaminidase activity (not shown), suggesting that these fractions contain the SG (Baram et al., 1999; Grimberg et al., 2003). However, probing the gradient fractions with the anti-Gα_{i2} antibody demonstrated that fractions 19-24 also contained p100, the Gi-related protein, which we have previously shown to localize to the recycling endosomes

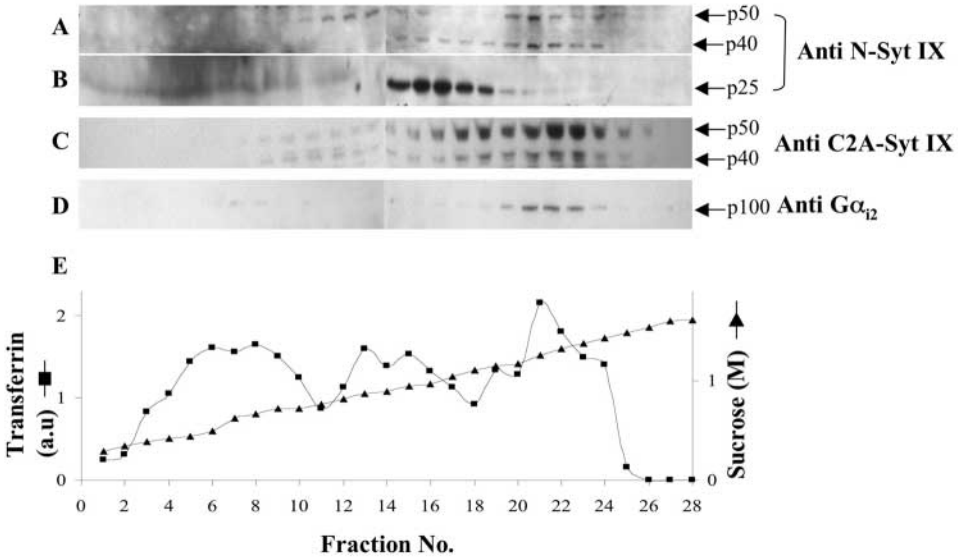

Fig. 3. Subcellular fractionation of RBL and RBL-Syt IX$^+$ cells. Cell homogenates derived from RBL (A,B,D,E) or RBL-Syt IX$^+$ (C) cells were fractionated on continuous sucrose gradients as described under Materials and Methods. Fractions were collected from the top, subjected to SDS-PAGE and immunoblotted with anti-N-Syt IX (A,B), anti-C2A-Syt IX (C) or anti-Gα_{i2} (D) antibodies as indicated. To monitor the distribution of internalized Tfn (E), RBL cells were serum starved for 1 hour followed by 1 hour of incubation with biotin-conjugated Tfn (20 μg/ml) at 37°C before fractionation. Fractions subjected to SDS-PAGE and immunoblotted with HRP-conjugated streptavidin, visualized by ECL and the intensities of the bands corresponding to biotin-Tfn were quantified by densitometry.

(Traub et al., 1990). Therefore, to confirm the association of recycling endosomes with these fractions, cells were allowed to internalize biotin-conjugated Tfn before fractionation on linear sucrose gradients. As shown in Fig. 3, biotin-Tfn was detected in 3 peaks. The first peak comigrated with light-density fractions that we have previously shown to contain the early endosomes (Grimberg at al., 2003). The second peak colocalized with the plasma membrane, whereas the third peak comigrated with p100 as well as with the 50/40 kDa Syt IX immunoreactive proteins (Fig. 3). These results therefore suggested that Syt IX may localize to either the SG or the recycling endosomes.

Visualization of Syt IX localization

To identify the cellular compartment with which Syt IX was associated we used confocal microscopy and the anti-C2A antibodies that react specifically with Syt IX. As shown in Fig. 4A, these antibodies stained a major perinuclear structure and also faintly stained the plasma membrane of RBL-Syt IX$^+$ cells. No granular pattern was detected, therefore excluding the SG as the site at which Syt IX resides. Notably, the anti-N-Syt IX antibodies also labeled a perinuclear structure in control RBL cells (Fig. 4B), consistent with the finding that the endogenous and overexpressed Syt IX colocalize (Fig. 3). However, these antibodies also labeled peripheral vesicles (Fig.

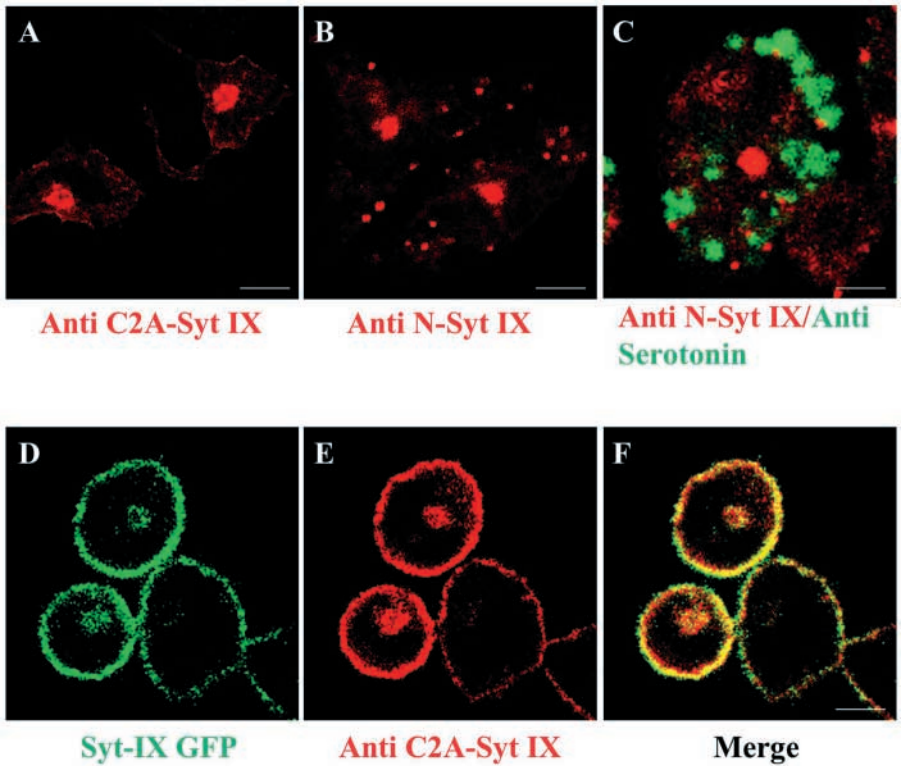

Fig. 4. Visualization of Syt IX localization. RBL-Syt IX$^+$ (A), control RBL (B,C) or RBL cells stably transfected with Syt IX-GFP cDNA (D-F) were labeled with anti-C2A-Syt IX (10 μg/ml) (A,D-F) or anti-N-Syt IX (10 μg/ml) alone (B), or together with mouse anti-serotonin (C) followed by rhodamine-conjugated donkey anti-rabbit and FITC-conjugated donkey anti-mouse IgG. Cells were processed for immunofluorescent staining and visualized by confocal microscopy, as described under Materials and Methods. Bars, 5 μm (A,B,D-F); 3 μm (C).

4B) that did not overlap with the SG marker serotonin (Fig. 4C), and their relevance to Syt IX is therefore currently uncertain.

We also investigated the localization of the GFP-tagged Syt IX protein in stably transfected RBL cells. Consistent with the localization of Syt IX in RBL-Syt IX$^+$ cells, Syt IX-GFP, detected by either its GFP fluorescence (Fig. 4D) or by staining with the anti-C2A antibodies (Fig. 4E), was distributed between the plasma membrane and the perinuclear structure (Fig. 4D-F).

Association of Syt IX with the ERC

We have previously shown that in RBL cells the ERC, to which internalized Tfn is delivered from the early endosomes (EE), is a perinuclear structure (Peng et al., 2002; Grimberg et al., 2003). Therefore we investigated whether Syt IX was localized to the ERC in the RBL cells. For this purpose, control and RBL-Syt IX$^+$ cells were allowed to internalize FITC-conjugated Tfn (FITC-Tfn) to label the ERC and Syt IX was labeled with either the anti-N-Syt IX antibodies in the control cells or with anti-C2A antibodies in the RBL-Syt IX$^+$ cells. As shown in Fig. 5, under these conditions internalized Tfn was delivered to a perinuclear structure where it significantly colocalized with Syt IX, stained with either antibody. Furthermore, Syt IX also colocalized with GFP-tagged Rab 11, a small GTPase known to associate with the ERC (Ren et al., 1998; Sheff et al., 1999; Trischler et al., 1999; Sonnichsen et al., 2000) (Fig. 5G-I).

To substantiate further the localization of Syt IX to the ERC rather than to the Golgi, we compared the effect of Brefeldin A (BFA), which causes collapse of the Golgi into the ER (Orci et al., 1991), on the localization of the Golgi marker mannosidase, Syt IX and internalized Tfn. Indeed, in sharp contrast to the Golgi enzyme mannosidase, whose perinuclear stain (Fig. 6C) was completely lost in BFA-treated cells (Fig. 6D), both Syt IX (Fig. 6A) and Tfn (Fig. 6E) also maintained their perinuclear localization in BFA-treated RBL cells (Fig. 6B,F).

Association of Syt IX with microtubules

ERC is made up of tubules assembled near the microtubule organizing center (MTOC) (Hopkins and Trowbridge, 1983). Indeed, double stain for Syt IX and tubulin demonstrated a complete overlap between the perinuclear localized Syt IX and the MTOC (Fig. 7A-D). Taxol treatment resulted in fragmentation of the MTOC and the concomitant formation of several tubulin clusters (Fig. 7F). In these cells, Syt IX translocated from its original perinuclear localization to the taxol-induced tubulin clusters (Fig. 7E,G). In marked contrast, both Tfn (Fig. 7I) and Rab 11 (Fig. 7J) were rather excluded

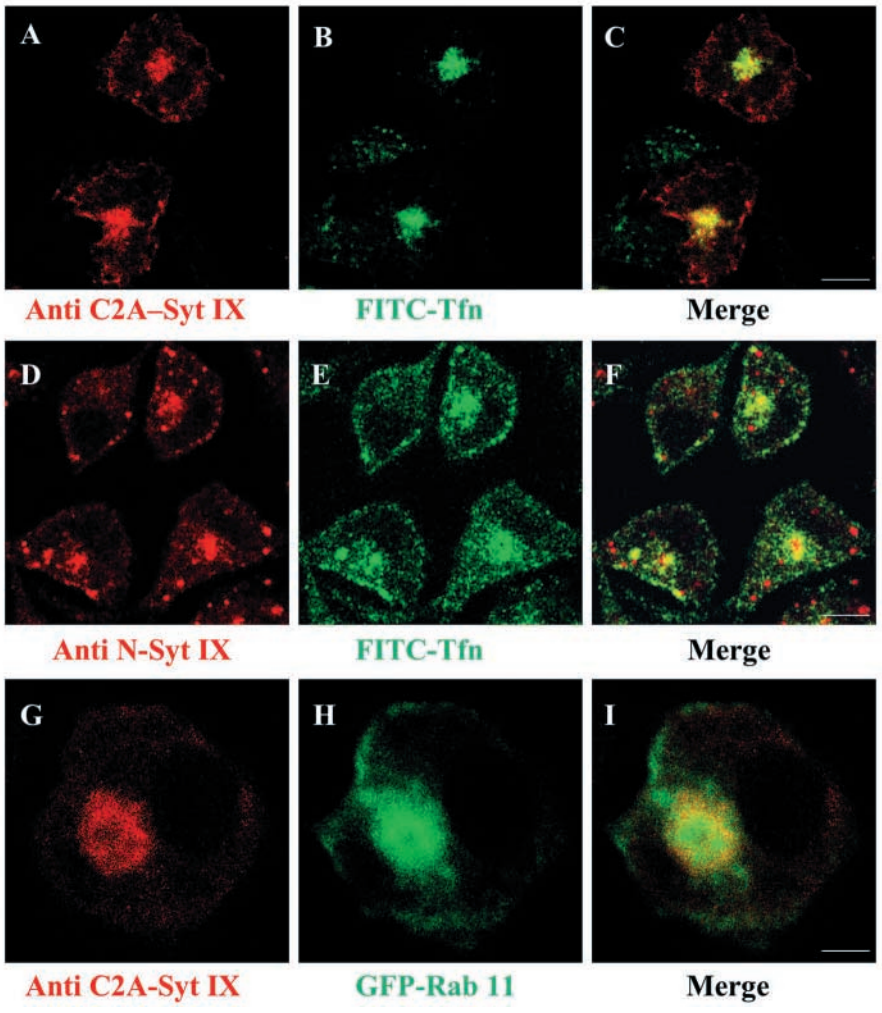

Fig. 5. Association of Syt IX with the ERC. RBL-Syt IX$^+$ cells (A-C,G-I) or control cells (D-F) were allowed to internalize FITC-conjugated Tfn for 30 (A-C) or 15 (D-F) minutes at 37°C, or were transiently transfected with Rab11-GFP cDNA (G-I). Cells were subsequently labeled with anti-C2A-Syt IX (A-C,G-I) or anti-N-Syt IX (D-F), followed by rhodamine-conjugated donkey anti-rabbit IgG. Bars, 5 μm (A-F); 3 μm (G-I).

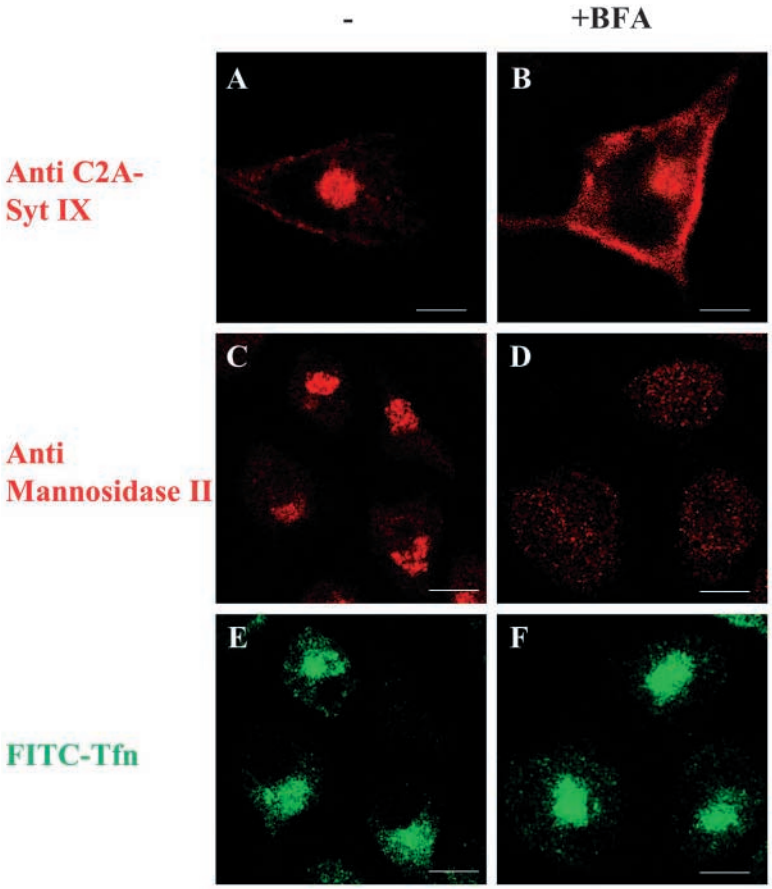

Fig. 6. Effect of BFA on Syt IX, internalized Tfn and mannosidase localization. RBL-Syt IX$^+$ cells were either untreated (A,C) or treated for 30 minutes at 37°C with BFA (5 μg/ml) (B,D), or allowed to internalize FITC-conjugated Tfn (50 μg/ml) for 1 hour (E,F) without (E) or with BFA (5 μg/ml) added for the last 30 minutes of Tfn internalization (F). Cells were subsequently labeled with either anti-C2A-Syt IX (A,B) or with anti-mannosidase II (C,D), followed by rhodamine-conjugated donkey anti-rabbit antibodies. Bars, 3 μm (A,B); 5 μm (C-F).

from these taxol-formed tubulin clusters. These results therefore suggested that under conditions in which taxol treatment prevented transport and fusion of EE-derived vesicles with the ERC, Syt IX-containing membranes remained associated with stabilized tubulin clusters.

Syt IX associates with tubulin both in vitro and in vivo

The close association between Syt IX and microtubules in both non-treated as well as taxol-treated cells suggested that Syt IX was able to interact with tubulin. To investigate this possibility, GST fusion proteins comprising either the C2A or C2B domains of Syt IX were used as affinity matrices and their ability to pull down tubulin from an RBL cell extract was evaluated. Both the C2A and the C2B domains pulled down both β (Fig. 8A) and α tubulin (Fig. 8B) in this in vitro assay. This binding required no Ca^{2+}, although Ca^{2+} significantly increased binding of tubulin by the C2A, but not the C2B domain (Fig. 8A,B). However, because only millimolar concentrations of Ca^{2+} affected tubulin binding to Syt IX-C2A, the physiological relevance of this finding is presently uncertain. Notably, neither the C2A nor the C2B domain of Syt IX bound any actin, suggesting that Syt IX may interact specifically with microtubules but not with microfilaments.

We could further demonstrate that Syt IX and tubulin co-immunoprecipitated from intact cells, thus indicating that Syt IX and tubulin also formed a complex in vivo. As shown in Fig. 9, an antibody directed against Syt IX was able to co-immunoprecipitate β tubulin (Fig. 9B), and conversely, anti-β tubulin co-immunoprecipitated Syt IX (Fig. 9C). This in vivo interaction did not require any Ca^{2+} and was not influenced by treating the cells with a Ca^{2+} ionophore (not shown).

Suppression of Syt IX slows recycling from the ERC

The localization of Syt IX to the ERC suggested that it might be involved in regulating transport to or from this compartment. To explore this possibility, we investigated if and how overexpression or suppression of Syt IX may affect the morphology, delivery to and export from the ERC. To this end we first monitored the internalization route of Texas Red-conjugated Tfn (TR-Tfn) in control (empty vector transfected), in Syt IX-overexpressing (RBL-Syt IX$^+$) and in Syt IX-suppressed (RBL-Syt IX$^-$) cells. Following 1 hour of incubation at 4°C, TR-Tfn was bound to the cell surface of all three cell-types (Fig. 10A-C), indicating that binding to the membranal Tfn receptor was not affected. To permit endocytosis the cells were warmed up and the uptake of Tfn was monitored. After 5 minutes of uptake, significant amounts of TR-Tfn were localized to small vesicles scattered throughout the cytoplasm in all three cell-types (Fig. 10D-F). These results therefore suggested that Syt IX was not required for the internalization of Tfn into the EE. After 30 minutes of uptake, most of TR-Tfn was found clustered around the cell nucleus (Fig. 10G-I), suggesting that Syt IX did not affect delivery to the ERC. Indeed, GFP-tagged Rab 11 transiently transfected into control, RBL-Syt IX$^+$ or RBL-Syt IX$^-$ cells, localized to the perinuclear region in all cell types (not shown).

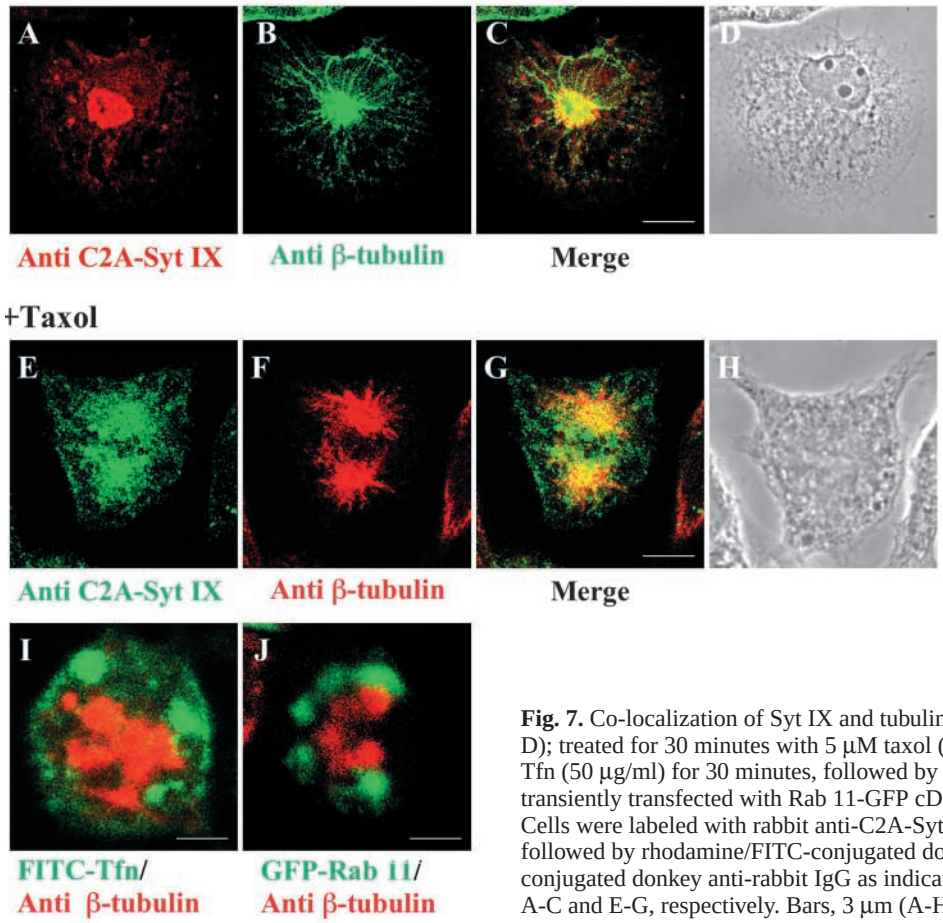

Fig. 7. Co-localization of Syt IX and tubulin. RBL-Syt IX$^+$ cells were: left untreated (A-D); treated for 30 minutes with 5 μM taxol (E-H); allowed to internalize FITC-conjugated Tfn (50 μg/ml) for 30 minutes, followed by 30 minutes of treatment with taxol (I); or transiently transfected with Rab 11-GFP cDNA and treated for 30 minutes with taxol (J). Cells were labeled with rabbit anti-C2A-Syt IX (A-H) or mouse anti-β-tubulin (A-J), followed by rhodamine/FITC-conjugated donkey anti-mouse IgG or rhodamine/FITC-conjugated donkey anti-rabbit IgG as indicated. D and H are the phase-contrast images of A-C and E-G, respectively. Bars, 3 μm (A-H); 2 μm (I,J).

Therefore modulation of Syt IX expression had no impact on the morphology or formation of the ERC.

Next we examined whether Syt IX affected the recycling of Tfn from the ERC to the cell surface. For this purpose, control, RBL-Syt IX$^+$ and RBL-Syt IX$^-$ cells were allowed to internalize TR-Tfn for 1 hour. The cells were subsequently washed and subjected to a chase in the presence of an excess of unlabeled Tfn. After a 30-minute chase, TR-Tfn was almost completely absent from both the control (Fig. 11E) and the RBL-Syt IX$^+$ cells (Fig. 11F). In sharp contrast, in the RBL-Syt IX$^-$ cells a large amount of TR-Tfn was retained (Fig. 11D). After a 1-hour chase most of TR-Tfn was also lost from the RBL-Syt IX$^-$ cells (Fig. 11G). Quantitative analysis of the average fluorescence intensity per cell for more than 100 cells revealed that ~30% of the total TR-Tfn were retained in RBL-Syt IX$^-$ cells at the end of the 30-minute chase, as opposed to only 15% that were retained in control and RBL-Syt IX$^+$ cells (Fig. 12). At the end of a 1-hour chase, 10-14% of Tfn were retained in all three cell-types (Fig. 12). These results therefore indicated that suppression of Syt IX substantially slowed the recycling of internalized Tfn from the ERC to the cell surface.

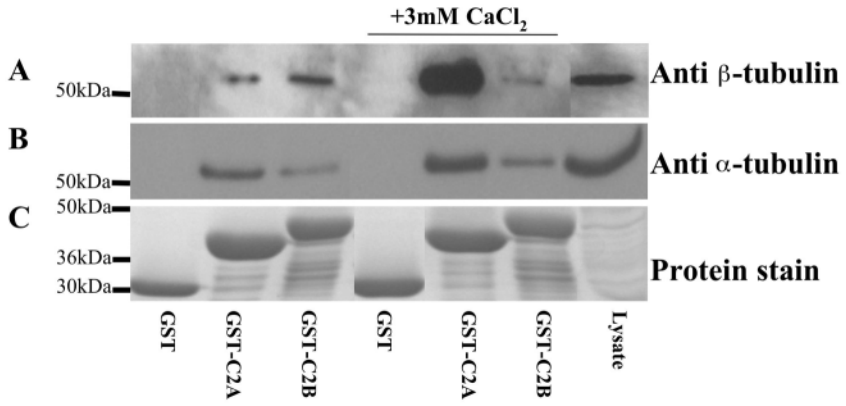

Fig. 8. Binding of tubulin by Syt IX. GST, GST-Syt IX-C2A or GST-Syt IX-C2B (20 μg) immobilized on glutathione sepharose beads were incubated for 4 hours at 4°C with RBL cell extracts (500 μg) as described under Materials and Methods, in the absence or the presence of Ca^{2+} (3 mM) as indicated. Bound proteins were eluted by sample buffer, resolved on SDS-PAGE and analyzed by either Western blot, using anti-α- or anti-β-tubulin antibodies, or by staining the gel with Coomassie blue as indicated.

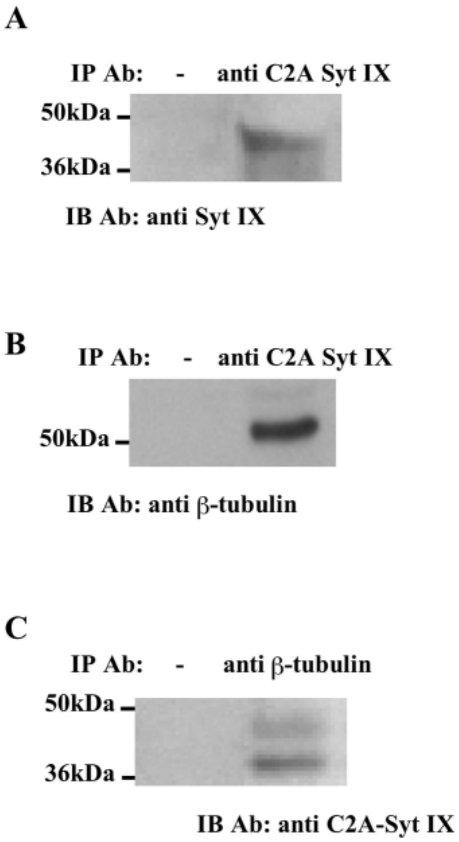

Fig. 9. Co-immunoprecipitation of Syt IX and tubulin from intact RBL cells. Immunoprecipitation was performed as described under Materials and Methods, using either the indicated immunoprecipitating antibody (IP Ab) followed by protein A Sepharose or incubated with protein A Sepharose without prior incubation with the primary antibody. Immune complexes were separated by SDS-PAGE and analyzed by Western blot using the indicated antibody (IB Ab).

Discussion

In this study we demonstrate that RBL cells endogenously express Syt IX. This finding extends our previous studies, in which we demonstrated that these cells endogenously express the Syt homologues Syt II, Syt III and Syt V (Baram et al., 1999). Syt IX, which shares the highest sequence similarity with Syt I and Syt II (Fukuda and Mikoshiba, 2001), was originally cloned from both human and rat cDNAs and named Syt V (Craxton and Goedert, 1995; Hudson and Birnbaum, 1995), although it was completely different in sequence from a different rat cDNA, which was also named Syt V (Li et al., 1995). Subsequently, two cDNAs were cloned from mouse, one of which was highly homologous to the human Syt V cDNA and it was termed Syt IX (Fukuda et al., 1999). Therefore, to date, the human, rat and mouse sequences are referred to as Syt IX (Craxton and Goedert, 1995; Hudson and Birnbaum, 1995; Fukuda et al., 1999), whereas the rat and mouse sequences remain Syt V (Li et al., 1995; Fukuda et al., 1999).

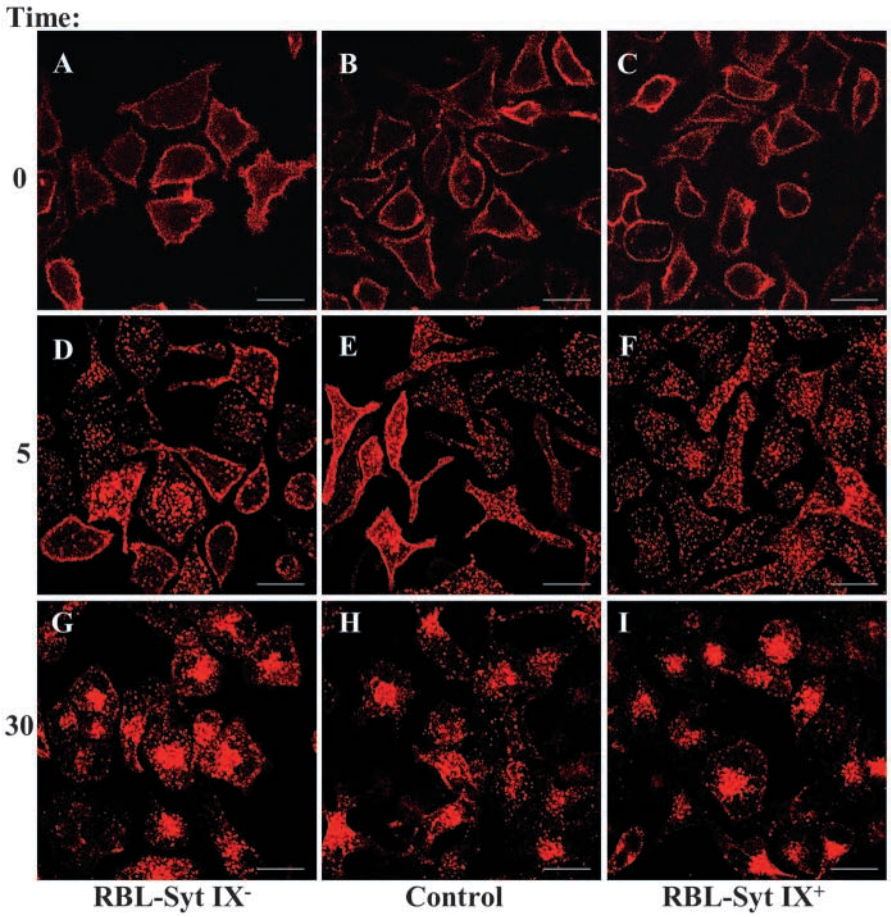

Fig. 10. Tfn internalization in control, Syt IX-overexpressing and Syt IX-suppressed RBL cells. RBL-Syt IX$^-$ (A,D,G), control (B,E,H) and RBL-Syt IX$^+$ (C,F,I) cells were grown on glass coverslips, serum starved for 1 hour and incubated with Texas-Red-conjugated Tfn (TR-Tfn, 50 μg/ml) for 1 hour at 4°C. Cells were subsequently left on ice (A-C) or warmed up to 37°C for 5 (D-F) or 30 (G-I) minutes. Cells were subsequently visualized by confocal microscopy as described under Materials and Methods. Bars, 13 μm.

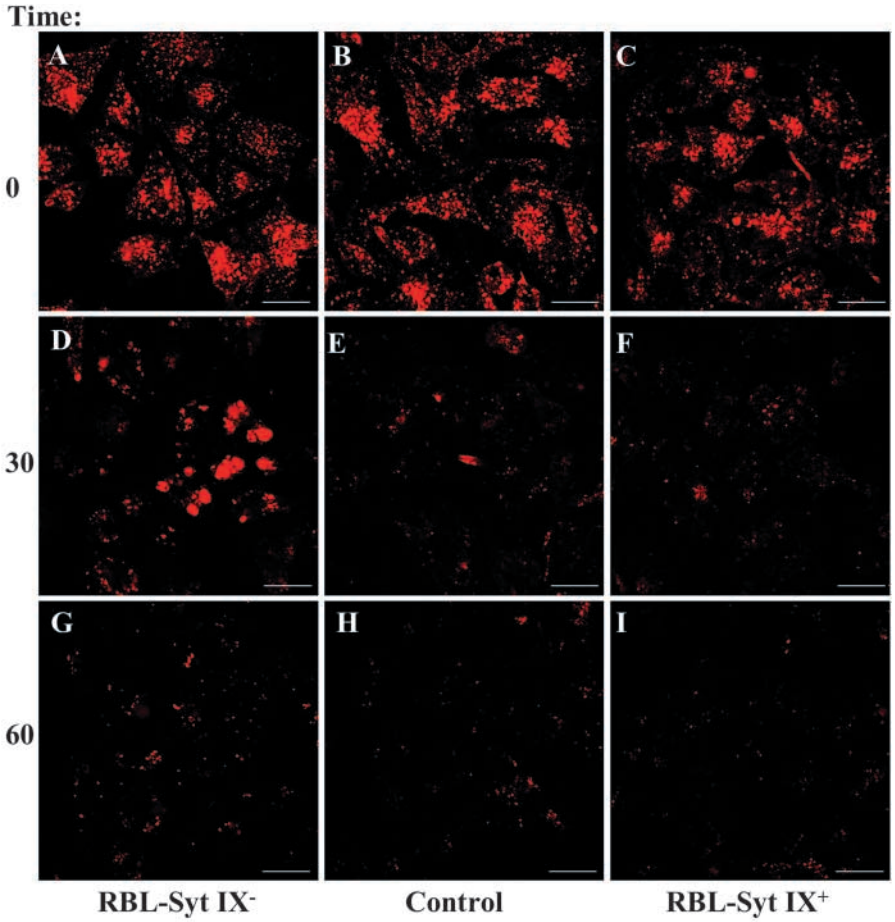

Fig. 11. Recycling of Tfn in control, Syt IX-overexpressing and Syt IX-suppressed RBL cells. RBL-Syt IX^{-} (A,D,G), control (B,E,F) and RBL-Syt IX^{+} (C,F,I) cells were grown on glass coverslips, serum starved for 1 hour and incubated with TR-Tfn (50 μg/ml) for 1 hour at 37°C. Cells were subsequently placed on ice (A-C) or washed and subjected to a chase in the presence of unlabeled Tfn (100 μg/ml) and defroxamine mesylate (100 μM) for 30 minutes (D-F) or 1 hour (G-I). Cells were processed and visualized by confocal microscopy, as described under Materials and Methods. Bars, 13 μm.

To characterize Syt IX at the protein level we used two antibodies that react specifically with Syt IX, one directed against an N-terminal sequence and the second against the C2A domain (Fukuda et al., 2002). The first antibody bound to three proteins (50, 40 and 25 kDa) present in RBL cells lysates (Fig. 2). However, although binding to all three proteins was specific and could be displaced by incubating the antibody with the immunizing peptide, only the expression level of the 50 and 40 kDa proteins was modulated upon transfecting the RBL cells with sense or antisense Syt IX cDNA, therefore questioning the relevance of the 25 kDa immunoreactive protein to Syt IX (Fig. 2).

The second anti-C2A antibody failed to detect the endogenous Syt IX, but did recognize the overexpressed 50 and 40 kDa proteins present in Syt IX-overexpressing cells (Fig. 2), therefore further supporting the notion that the 25 kDa immunoreactive protein is probably unrelated to Syt IX. Whether the 50 and 40 kDa immunoreactive proteins represent two differently post-translationally modified forms of Syt IX or whether the 40 kDa is a degradation product is presently unknown.

Because of the cross-reactivity of the anti-N-Syt IX antibodies with the 25 kDa Syt IX-unrelated protein, it was necessary to use the anti-C2A antibodies and Syt IX-overexpressing cells (RBL-Syt IX^{+}) to define the cellular localization of Syt IX. Therefore we first investigated whether the overexpressed and the endogenous Syt IX protein(s) were indeed targeted to the same intracellular localization. This was achieved by fractionating control and RBL-Syt IX^{+} cells on linear sucrose gradients and comparing the migration of the 50/40 kDa proteins recognized by the anti-N-ter antibodies in control cells with that of the 50/40 kDa proteins recognized by the anti-C2A antibodies in the RBL-Syt IX^{+} cells. Indeed, this analysis confirmed that both the transfected and the endogenous Syt IX are associated with similar fractions that also contain the SG and the recycling endosomes (Fig. 3).

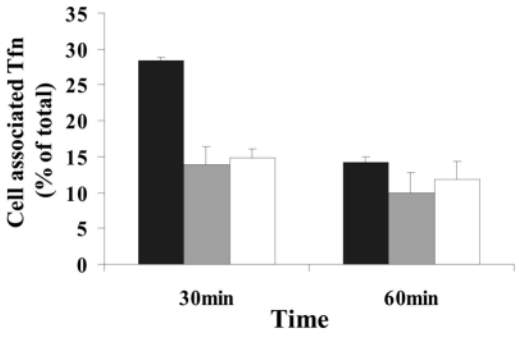

Fig. 12. Quantitative analysis of fluorescence images of Tfn recycling in control, Syt IX-overexpressing and Syt IX-suppressed RBL cells. The average fluorescence intensity per cell was measured for more than 100 cells per each condition described under Fig. 11.

However, visualization of Syt IX using the anti-C2A antibodies revealed that Syt IX localizes mainly to a single perinuclear structure where it significantly overlaps with both internalized Tfn and Rab11 rather than with serotonin-containing vesicles (Fig. 4). Hence, in marked contrast to Syt IX localization in PC12 cells where it localizes to the dense-core secretory vesicles (Fukuda et al., 2002), in RBL cells Syt IX localizes to the ERC. In the RBL-Syt IX$^+$ cells, Syt IX was also detected at the plasma membrane (Figs 3, 4). This observation raises the possibility that the plasma membrane is an intermediate in the biosynthetic route of Syt IX, or that Syt IX function involves cycling between the ERC and the cell surface.

The ERC that is involved in receptor and lipid recycling (Nichols et al., 2001) is characterized by its tubulovesicular morphology and dependence on intact microtubules for localization (Hopkins and Trowbridge, 1983). In particular, the perinuclear endocytic recycling compartment is clustered around the centrosome, where it is tightly associated with the MTOC. Indeed, Syt IX also colocalizes with tubulin at the MTOC (Fig. 7). Moreover, several observations indicate that Syt IX is tightly associated with tubulin. First, Syt IX remains associated with tubulin clusters formed in taxol-treated cells (Fig. 7). This is in sharp contrast to Tfn or Rab 11 that are rather excluded from tubulin in taxol-treated cells (Fig. 7). Second, Syt IX co-immunoprecipitates with tubulin from intact cells (Fig. 9), and finally, chimeric GST fusion proteins, comprising the C2A or C2B domains of Syt IX, bind tubulin in pull-down assays (Fig. 8). Thus, unlike Syt I, which requires Ca^{2+} concentrations in the millimolar range to bind tubulin (Honda et al., 2002), Ca^{2+} is not required for tubulin binding by Syt IX. However, it is important to note that although our data clearly establish an association between Syt IX and tubulin, this association might be indirect and involve intervention by as yet unidentified adaptor proteins.

The localization of Syt IX to the ERC and its ability to associate with tubulin have raised the possibility that Syt IX might play a role in linking or coordinating ERC-dependent transport with the microtubules. Previous studies have demonstrated that the export of cargo from the ERC to the cell surface depends on microtubules (Lin et al., 2002). This, together with our observation that in overexpressing cells Syt IX can also be detected at the plasma membrane, therefore suggested that Syt IX may control microtubules-dependent recycling from the ERC. To explore this possibility we compared the recycling process of internalized Tfn in control, RBL-Syt IX$^+$ and RBL-Syt IX$^-$ cells. Our results provide unequivocal evidence for an active role for Syt IX in controlling the export from the ERC to the cell surface. We demonstrate that suppression of Syt IX by 90% by stable transfection with Syt IX antisense cDNA significantly decreases the rate of Tfn recycling (Figs 11, 12). Notably, this effect is specific as neither internalization of Tfn from the plasma membrane to the EE, nor the delivery of Tfn or recruitment of Rab 11 to the ERC are affected by Syt IX suppression. This is in marked contrast to Syt III, whose suppression prevented Tfn and Rab 11 from reaching the ERC (Grimberg et al., 2003). Based on the active role of Syt IX in controlling export from the ERC together with its ability to associate with tubulin, we hypothesize that Syt IX may play a role in linking ERC-dependent transport with the microtubules.

In conclusion, our results provide further support for the notion that non-neural Syts display distinct cellular localizations and unique functions. Specifically, we have previously shown that Syt III regulates delivery of internalized Tfn from the EE to the ERC (Grimberg et al., 2003), and we now show that Syt IX regulates the export of internalized Tfn from the ERC to the cell surface.

We thank Dr L. Mittelman for his invaluable help in all the laser confocal microscopy studies. We thank Drs Y. Zick, D. Neumann and K. Hirschberg for helpful discussions and a critical reading of this manuscript, and Drs M. Zerial, A. Spiegel and J. Donaldson for their generous gifts of cDNAs and antibodies. Supported by grants from the Israel Science Foundation, founded by the Israel Academy for Sciences and Humanities, by the Israel Ministry of Health (R.S.-E.) and the Constantiner Institute (Y.H. and E.G.).

References

Aruffo, A. and Seed, B. (1987). Molecular cloning of a CD28 cDNA by the high-efficiency COS cell expression system. *Proc. Natl. Acad. Sci. USA* **84**, 8573-8577.

Baram, D., Adachi, R., Medalia, O., Tuvim, M., Dickey, B., Mekori, Y. and Sagi-Eisenberg, R. (1999). Synaptotagmin II negatively regulates Ca^{2+}-triggered exocytosis of lysosomes in mast cells. *J. Exp. Med.* **189**, 1649-1658.

Chapman, E. R. (2002). Synaptotagmin: a Ca^{2+} sensor that triggers exocytosis? *Nat. Rev. Mol. Cell Biol.* **3**, 498-508.

Craxton, M. and Goedert, M. (1995). Synaptotagmin V: a novel synaptotagmin isoform expressed in rat brain. *FEBS Lett.* **361**, 196-200.

Fukuda, M. and Mikoshiba, K. (2000). Distinct self-oligomerization activities of synaptotagmin family: unique calcium-dependent oligomerization properties of synaptotagmin VII. *J. Biol. Chem.* **275**, 28180-28185.

Fukuda, M. and Mikoshiba, K. (2001). Characterization of KIAA1427 protein as an atypical synaptotagmin (Syt XIII). *Biochem. J.* **354**, 249-257.

Fukuda, M., Kanno, E. and Mikoshiba, K. (1999). Conserved N-terminal cysteine motif is essential for homo- and heterodimer formation of synaptotagmins III, V, VI, and X. *J. Biol. Chem.* **274**, 31421-31427.

Fukuda, M., Kojima, T. and Mikoshiba, K. (1996). Phospholipid composition dependence of Ca^{2+}-dependent phospholipid binding to the C2A domain of synaptotagmin IV. *J. Biol. Chem.* **271**, 8430-8434.

Fukuda, M., Kowalchyk, J. A., Zhang, X., Martin, T. F. and Mikoshiba, K. (2002). Synaptotagmin IX regulates Ca^{2+}-dependent secretion in PC12 cells. *J. Biol. Chem.* **277**, 4601-4604.

Grimberg, E., Peng, Z., Hammel, I. and Sagi-Eisenberg, R. (2003). Synaptotagmin III is a critical factor for the formation of the perinuclear endocytic recycling compartment and determination of secretory granules size. *J. Cell Sci.* **116**, 145-154.

Honda, A., Yamada, M., Saisu, H., Takahashi, H., Mori, K. J. and Abe, T. (2002). Direct Ca^{2+}-dependent interaction between tubulin and synaptotagmin I: a possible mechanism for attaching synaptic vesicles to microtubules. *J. Biol. Chem.* **277**, 20234-20242.

Hopkins, C. R. and Trowbridge, I. S. (1983). Internalization and processing of transferrin and the transferrin receptor in human carcinoma A431 cells. *J. Cell Biol.* **97**, 508-521.

Hudson, A. W. and Birnbaum, M. J. (1995). Identification of a nonneuronal isoform of synaptotagmin. *Proc. Natl. Acad. Sci. USA* **92**, 5895-5899.

Li, C., Ullrich, B., Zhang, J. Z., Anderson, R. G. W., Brose, N. and Sudhof, T. C. (1995). Ca(2+)-dependent and -independent activities of neural and non-neural synaptotagmins. *Nature* **375**, 594-599.

Lin, S. X., Gundersen, G. G. and Maxfield, F. R. (2002). Export from pericentriolar endocytic recycling compartment to cell surface depends on stable, detyrosinated (glu) microtubules and kinesin. *Mol. Biol. Cell* **13**, 96-109.

Nichols, B. J., Kenworthy, A. K., Polishchuk, R. S., Lodge, R., Roberts, H., Hirschberg, K., Phair, R. D. and Lippincott-Schwartz, J. (2001). Rapid cycling of lipid raft markers between the cell surface and Golgi complex. *J. Cell Biol.* **153**, 529-541.

Orci, L., Tagaya, M., Amherdt, M., Perrelet, A., Donaldson, J., Lippincott-Schwartz, J., Klausner, R. D. and Rothman, J. E. (1991). Brefeldin A, a drug that blocks secretion, prevents the assembly of non-clathrin-coated buds on Golgi cisternae. *Cell* **64**, 1183-1195.

Peng, Z., Grimberg, E. and Sagi-Eisenberg, R. (2002). Suppression of Synaptotagmin II restrains phorbol ester-induced down-regulation of protein kinase Cα by diverting the kinase from a degradative pathway to the recycling endocytic compartment. *J. Cell Sci.* **115**, 3083-3092.

Ren, M., Xu, G., Zeng, J., De, L. C. C., Adesnik, M. and Sabatini, D. D. (1998). Hydrolysis of GTP on rab11 is required for the direct delivery of transferrin from the pericentriolar recycling compartment to the cell surface but not from sorting endosomes. *Proc. Natl. Acad. Sci. USA* **95**, 6187-6192.

Saegusa, C., Fukuda, M. and Mikoshiba, K. (2002). Synaptotagmin V is targeted to dense-core vesicles that undergo calcium-dependent exocytosis in PC12 cells. *J. Biol. Chem.* **277**, 24499-24505.

Sheff, D. R., Daro, E. A., Hull, M. and Mellman, I. (1999). The receptor recycling pathway contains two distinct populations of early endosomes with different sorting functions. *J. Cell Biol.* **145**, 123-139.

Shin, O. H., Rizo, J. and Sudhof, T. C. (2002). Synaptotagmin function in dense core vesicle exocytosis studied in cracked PC12 cells. *Nat. Neurosci.* **5**, 649-656.

Sonnichsen, B., De, R. S., Nielsen, E., Rietdorf, J. and Zerial, M. (2000). Distinct membrane domains on endosomes in the recycling pathway visualized by multicolor imaging of Rab4, Rab5, and Rab11. *J. Cell Biol.* **149**, 901-914.

Sugita, S., Shin, O. H., Han, W., Lao, Y. and Sudhof, T. C. (2002). Synaptotagmins form a hierarchy of exocytotic Ca^{2+} sensors with distinct Ca^{2+} affinities. *EMBO J.* **21**, 270-280.

Traub, L. M., Evans, H. W. and Sagi-Eisenberg, R. (1990). A novel 100 kDa protein, localized to receptor enriched endosomes, is immunologically related to the signal transducing G proteins Gt and Gi. *Biochem. J.* **272**, 453-458.

Trischler, M., Stoorvogel, W. and Ullrich, O. (1999). Biochemical analysis of distinct Rab5- and Rab11-positive endosomes along the transferrin pathway. *J. Cell Sci.* **112**, 4773-4783.